

Exploring the Gauge Hierarchy Problem at $N = 2$ with TeV^{-1} -sized Black Holes

Jason Minamora^{1,2}

¹*California Institute of Technology, Department of Physics, Mailcode 356-48, 1200 E. California Blvd., Pasadena, CA 91125*

²*Institute of Geophysics and Planetary Physics, University of California, Los Angeles, Box 951567, Los Angeles, CA 90095*

Abstract

A mass Hierarchy of magnitude $O(10^{16})$ GeV separates the gravitational and electroweak interactions. Traditional proposed resolutions of this anomaly have included supersymmetric theories (most notably, the MSSM and ESSM) and string theory. However, energies at which supersymmetric particles are expected to appear are not accessible to experiment, and string theory is only testable at $\sim M_{\text{Pl}}$. A novel idea involves introducing extra dimensions into a Minkowski space-time to reduce the effective separation between the gauge and gravitational couplings. Theoretical developments of the so-called Arkani-Dinopolous-Dvali (ADD) extra-dimensional scenario, and its experimental verification, are presented here.

1 Background

The gap between the strengths of the electromagnetic and gravitational interactions places constraints on the applicability of the Standard Model (SM). The cutoff scale between the gauge ($M_{\text{EW}} = 10^3$ GeV) and gravitational forces ($M_g \approx M_{\text{Pl}} = 10^{19}$ GeV) is large [1] ($\Lambda \sim 10^{16}$), suggesting a necessary extension to the SM.

Supersymmetric extensions to the SM have been proposed to resolve the gauge hierarchy. The Minimal Supersymmetric Standard Model (MSSM)—see, for example, [2]—assigns fermion superpartners to gauge bosons (including the unseen Higgs), and the spin- $\frac{3}{2}$ gravitino to the graviton. These particles, however, are yet to be seen; see Table 1, and also ref. [3] for discussion.

SM Particle(s)	MSSM Counterpart(s)	UL(MSSM) [GeV] (CL = 95%)
γ, Z^0, H^0	$\tilde{\chi}_i^0$ (neutralinos)	66.4
W^\pm, H^\pm	$\tilde{\chi}_i^\pm$ (charginos)	67.7
e	\tilde{e}	95.0
g	$\tilde{\chi}_g$ (gravitino)	(no data)

Table 1: Upper limits on MSSM particle searches. Note that all values are within experimental reach. Values taken from ref. [4].

An alternative approach to the problem (discussed here) is to introduce extra spatial dimensions, each of radius R . In this scheme, the Planck scale is no longer fundamental. Instead, a test mass m will experience a potential

$$V(r) = \frac{m}{M_*^{N+2} R^N} \frac{1}{r} \quad (r \gg R) \quad (1)$$

a distance r from the source. M_{Pl} is now replaced with the effective $(4 + N)$ -dimensional Planck mass [5]:

$$M_{\text{Pl}}^2 = M_*^{2+N} R^N.$$

If we choose $M_* \approx M_{\text{EW}}$, then gravity is of the same order as the gauge forces; substituting in figures gives

$$R \approx 10^{\frac{30}{n}-17} \times \left(\frac{1 \text{ TeV}}{m_{\text{EW}}} \right)^{\frac{2}{n}+1}.$$

The distance scale for $N = 1$ is too large— $R = 1 \text{ AU}$. The $N = 2$ case, which gives TeV^{-1} (millimeter-) sized R , is empirically accessible [6].

One of the more interesting implications from the $N = 2$ theory is production (and decay) of millimeter-sized black holes (BHs) at experiments [7, 8]. The simplest scenario arises when one considers Hawking-type BHs. From a classical, two-dimensional viewpoint [9], Hawking black holes decay forever. In $(4 + 2)$ dimensions, the BH lifetime can be taken to be instantaneous. This is convenient, since one can produce and compare the decay spectrum of $N = 2$ BHs against the (higher-dimensional) Hawking spectrum in a short time. If BH branching fractions agree with those predicted by the Hawking model, a new upper limit could be placed on the quantum gravity scale.

2 Phenomenological Considerations

The simplest description of a Hawking BH is the semiclassical one, valid for masses $M_{\text{BH}} \gg M_*$.¹ The semiclassical approximation fails, however, when $M_{\text{BH}} \sim M_*$, since stringy corrections are no longer negligible. For our purposes, though, we will restrict discussion to the former case, where the spectroscopy of BH decays is well-described [10].

Production and Decay of TeV^{-1} -sized Black Holes

If BHs are produced with masses much larger than M_* , the Schwarzschild radius R_s can be found using classical considerations [11]. For the six-dimensional case,

$$R_s = \pi^{-1/3} \left(\frac{3M_{\text{bh}}}{2M_*} \right)^{\frac{1}{3}} \frac{1}{M_*}. \quad (2)$$

In particular, a reduced mass M_* of 1 TeV places an upper limit on the size of these objects in the millimeter range, for production energies of up to $\sim 10 \text{ TeV}$. These energies are presently above the thresholds of experiment, but the mechanism for production is still valid.

Consider the parton-parton² scattering process shown in Fig. 1. Such reactions may take place at the LHC, and in collisions between neutrinos and baryons. If the impact parameter $R_s(\hat{s})$ is smaller than R_s , we expect a vortex—here, a black hole—to form [8].

In our approximation, millimeter-sized black holes decay via the Hawking spectrum [12],

$$\frac{dN_i}{dt} \sim \frac{\Gamma_s(E, s)}{e^{E/T} - (-1)^{2s}} \frac{d^5 k}{(2\pi)^5}. \quad (3)$$

The *greybody factor* Γ_s is dependent on both the spin s , and the energy E ; Γ_s , then, is effectively an absorption cross-section for particle species i . Because the Hawking distribution law (3) contains a term in the (normalized) five-momentum, $d^5 k$, we see that energy is radiated faster from a TeV^{-1} -sized black hole, than from a classical Schwarzschild black hole, because of the increased phase-space volume available to the decaying particle. In fact, lifetimes for the six-dimensional case are approximately 1 fs.

Expression (3) bears resemblance to the Planck distribution function for a classical blackbody radiator:

$$\frac{dN(\lambda, T)}{dE} \sim \frac{1}{(\lambda T)^2} \frac{1}{e^{1/\lambda k T} \pm 1}. \quad (4)$$

¹Here, M_* is the $N = 2$ effective Planck mass.

²The six quarks and gluons.

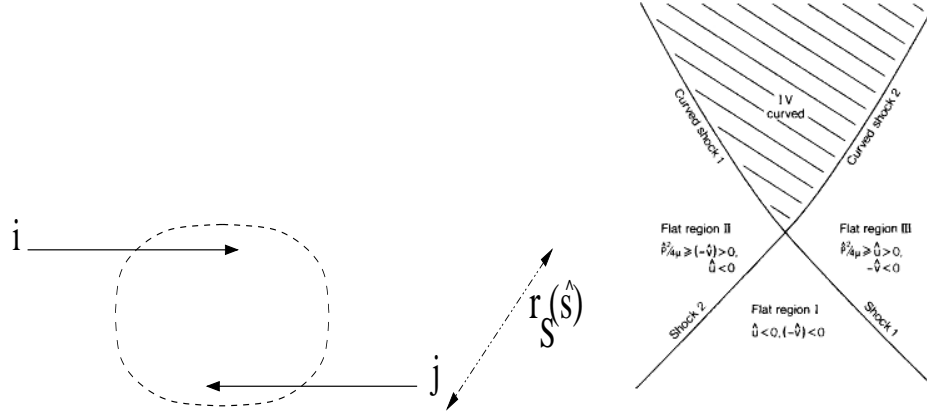


Figure 1: Parton scattering. (1A—Left) Close-range interactions between two partons i and j produce a vortex of size $\sim r_S(\hat{s} = E_{\text{cm}})$. (1B—Right) The topological profile of space changes abruptly near the scattering region. Regions (I), (II) and (III) fall outside the area cartooned in Fig. 1A; space there is flat ($g_{\mu\nu} = \eta_{\mu\nu}$). In the production region (IV), the metric may be of Schwarzschild form, with a singularity at the center.

The prefactor in λ^{-2} indicates that (4) is valid in the three-dimensional case (if we identify the de Broglie momentum $p = 1/\lambda$). Classical BHs are, therefore, longer-lived than those in six-dimensional space. Consequently, the momentum factor in (3) suggests that millimeter-sized black holes decay into dominantly soft components (such as jets) compared to the macroscopic case (4).

One major obstacle is controlling Standard Model (SM) background. Because the interaction between partons is mediated by either a γ , W^\pm , or Z^0 , there may be a contribution from the mode $Z^0 \rightarrow e\bar{e}$ to the leptonic component of the spectrum.

Simulation of Black Hole Events

The scattering process outlined in Fig. 1 is the primary means for producing black holes at the LHC and elsewhere [7, 8, 12]; software to simulate the interaction has already been constructed [13]. Current simulation techniques model parton evolution from pp and $p\bar{p}$ processes—those most often studied at the LHC.

The software used to predict the decay products of black holes is not subject to the two major constraints of the theory outlined above; modern BH event generators include analyses of time-varying behavior—that is, temperature and spectroscopy—and attempts to describe the terminal state of BH decay. One shortcoming of the semiclassical approximation is a steady-state model that assumes equal branching fractions for all of the 60 particles in the SM [5]; that assumption is relaxed in a stochastic model, since the greybody factor Γ_s is a free parameter in the simulation. Table 2 shows results from a Monte-Carlo run using the CHARYBDIS analysis package [14].

3 Experimental Foundations (Proposed)

A host of ground-based and fixed-target experiments plan to begin searches for black holes once TeV physics is empirically realized. Among these are the LHC [7, 8] (which will include the ATLAS detector [15]), and AMANDA/ICECUBE [13, 16, 17].

Species	Energy [GeV]	
	Est. Mean (± 50 GeV)	Est. 90% UL (± 50 GeV)
H^0	500	1250
e^\pm	500	1250
γ	650	1200

Table 2: Mean values and 90% upper limits on energy for simulated decay spectra. Values taken from [14].

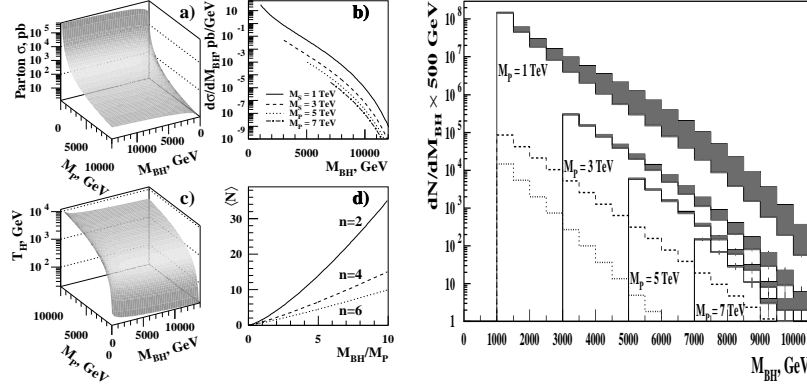


Figure 2: (2A—Left) Scale-dependent parton cross-sections [subpanel (a)] and simulated multiplicity data [subpanel (d)] LHC collisions ($\sigma_{\text{incl.}} = 1$ mb) should indeed produce BHs at a rate Γ_{BH} if they are seen, and are found to decay via the Hawking mechanism. (2B—Right) Simulated number of BH events per unit reduced Planck mass, for four different values of M_{BH} . Shaded regions give ranges for $2 \leq N \leq 7$. Dashed and dotted lines are expected contributions from the background modes $\Gamma(Z^\circ \rightarrow \ell^\pm \nu) + \Gamma(Z^\circ \rightarrow \gamma + X)$, and $\Gamma(Z^\circ \rightarrow \gamma + X)$ only, respectively [9].

Partonic scattering at the LHC

Proton-anti-proton scattering with center-of-mass energy E_{cm} greater than the $N = 2$ BH production threshold M_{BH} can be done with current experimental thresholds. experiment. If BHs are produced, they will be produced copiously at the LHC.

Collider experiments have already established empirical lower limits on center-of-mass production energies; the most recent summary reports a 1.3-TeV threshold for the $N = 2$ case. This is below the phenomenological limit derived from the higher-dimensional Newton's constant, however ($E_{N=2} \gtrsim 1.6$ TeV), and so searches in higher-energy regimes still look promising [18].

The LHC collider beams are tentatively scheduled to operate at 7.0 TeV, with $\sim 1 \times 10^{14}$ collisions per second. The BH production rate, Γ_{BH} , depends on $\sqrt{\hat{s}_{\text{beam}}}$, the collision rate, and a composite efficiency $\epsilon = \epsilon_b \times \epsilon_1$, based on beam injection parameters and predicted losses during operation. Estimates using simulated protons at injection and during procession around the LHC storage ring give efficiencies between 10^{-5} and 10^{-4} [19]; we therefore expect $\Gamma_{\text{BH}}(p\bar{p} \rightarrow BH) \lesssim 10^{10} \text{ s}^{-1}$; simulated BH production cross-sections give similar predictions; see Fig. 2A.

ATLAS, which uses the $p\bar{p}$ beam, plans to take its first science run in 2007. The proposed detector will be sensitive to leptonic and electromagnetic decays from hard scattering events; efficient detection of ℓ and γ tracks is important for reconstructing BH decay products, since the observable portion of the Hawking spectrum is dominated by the intermediate vector bosons and charged leptons—see Table 4. One must also be clever in separating SM background events due to the decay of the Z° , since products from leptonic decay channels may appear as BH signal. This background can be significant, as shown in Fig. 2B. Obtaining

accurate counts from electromagnetic processes also presents difficulty, because of large photon multiplicities from pseudoscalar meson decays—some examples of more exotic decays with significant electromagnetic contributions are shown in Table 3. Placing kinematic cuts on mass differences between particles and decay products is a straightforward way to crudely correct for SM events.

Selected $p\bar{p}$ Scattering Modes		
	Primary Decay	Final State
$p\bar{p} \rightarrow 3\pi^0$	$3\pi^0$	6γ
$p\bar{p} \rightarrow 2\pi^0 + X$	$\pi^0\pi^0\eta'$	$10\gamma, 6\gamma$
	$\pi^0\pi^0\omega$	7γ
	$\pi^+\pi^-\eta'$	$\pi^+\pi^-16\gamma$ (Dominant)
n $p\bar{p} \rightarrow \pi^0 + X$	$\pi^0\omega\eta$	7γ
	$\pi^0\eta\eta$	6γ
	$\pi^0\eta\eta'$	6γ

Table 3: Electromagnetic $p\bar{p}$ channels with potential, non-trivial contributions to the γ component of the BH Hawking decay spectrum. Many such secondary decays are expected to be seen at the LHC; see ref. [20] for a full account.

Cosmic-Ray Production of BHs

Ultra-high-energy photons from extragalactic sources produce neutrinos in matter, which are readily available for detection by ground-based detectors. The parton scattering model discussed earlier can similarly be used here to discuss BH production in extensive air showers. Photons that initiate electromagnetic cascades are typically in the range 10^{15} – 10^{21} eV. For reasons to be discussed below, ground-based detectors have the highest likelihood of seeing BH events, because of the low background. Neutrino arrays are sensitive to the highest-energy portions of the cascade spectrum; BH formation should thus take place simultaneously with presently observed neutrino-matter interactions. If BHs are to be produced via parton interactions, then the reaction $\nu N \rightarrow BH + \mu^\pm \ell^\mp X$ warrants consideration. Expected BH event rates (based on the ADD scenario [11]) for the South Pole-based ICECUBE neutrino array have been calculated based on cosmic neutrino fluxes [7, 11]:

$$\begin{aligned}\Gamma_{\text{BH}} &= \int N(E) \frac{d\sigma}{d\Omega} d\Omega = n_p \times \int_{M_*}^{E_{\text{max}}^\nu} \frac{d\sigma}{dE} \Phi(E) dE \\ &= (3.5 \times 10^{-35}) N \quad (\text{events/yr}).\end{aligned}\tag{5}$$

Here, $\sigma = \sigma(E)$ is the ADD-estimated cross-section for particle fluxes $\Phi(E)$. For $N = 10^{39}$, the number of protons in 1 km^3 of ice, ~ 100 BHs per day should be seen from neutrino-nucleon scattering at ICECUBE.³

Cosmic-ray experiments offer a distinct advantage over beam-beam collision facilities like the LHC: the freedom to choose between different active sources at various distances from Earth makes background correction a very simple task. Figure 3 shows the signal-to-noise ratio plotted against kinematic and spatial parameters. Depending on the intensity of the source, background begins to dominate at some critical distance d_c (Fig. 3A). For objects at distances $d < d_c$, the effective area of air showers fully covers the field of view of the detector; background is no longer significant, allowing easy reconstruction of decay matter from BHs. Fig. 3B takes the form of a “rate-versus-threshold” curve: signal is ultimately detector-limited, and is seen to level off at Lorentz factors $\gamma \sim 450$. However, the shape of such a curve does not yield much scientific information, since it is the choice of threshold energy that determines photomultiplier tube response to cascades. The spectral profile of gamma-ray bursts (GRBs) can be directly extracted from Fig. 3C; low

³The rate calculated from (5) is for a six-dimensional BH (the $N = 2$ case).

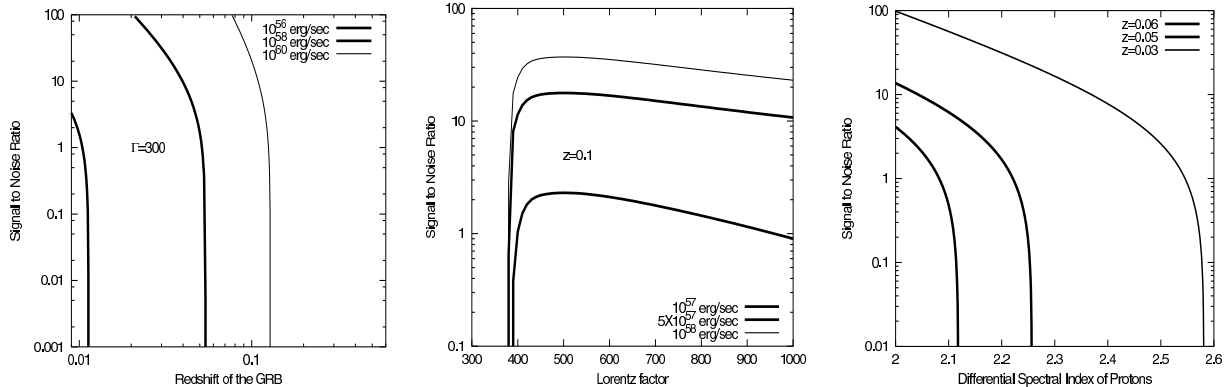


Figure 3: Signal-to-noise ratio for ICECUBE-type detectors. Three regimes are shown, for three different values of the luminosity—dependence on distance (3A, left), outflow velocity (3B, center), and spectral index (3C, right) [17]. These plots correspond to a 250 GeV threshold; normal incidence is assumed.

levels of signal from far away sources in higher-energy regions ($\alpha \gtrsim 2.4$) can be attributed to attenuation effects; ICECUBE is sensitive to the hard component of the spectrum for GRBs that are relatively nearby (dotted line in Fig. 3C). Using ICECUBE as a nominal example of large-scale ground-based detectors, we find that such detectors' ability to observe sources at a continuum of distance scales, and their freedom to discriminate at different thresholds, results in background minimization superior to fixed-target and beam-beam experiments. So far, black holes have not yet been observed in the mode $\nu N \rightarrow \text{BH} + X$; upper limits are given elsewhere [21]. Should one be produced, scintillations from heavier decay products (W^\pm, ℓ) will be seen in the ice, even though semi-classical arguments include all SM particles in the BH decay spectrum. Unlike the LHC, ground-based detection enjoys a high signal-to-noise ratio, and should therefore be sensitive to not only the quarks and leptons (see Table 4), but also the more exotic SM particles. It is likely that the first BH event will be seen in cosmic-ray apparatuses.

	q	ℓ	g	W^\pm, Z	γ	G^0, G^\pm	H
Relative Contribution(%)	52.94	17.65	17.65	6.62	2.21	2.21	0.74

Table 4: Relative contributions of SM constituents to the Hawking Decay Spectrum. Values derived from multiplicity data given in [12].

4 Summary and Conclusion

Higher-dimensional theories can be used to bridge the gap between the electroweak (gauge) interactions and gravity. We have considered one such application that introduces extra TeV^{-1} (mm) -sized dimensions into space, which in turn lowers the fundamental Planck scale M_* to within experimental bounds. Observing Black holes in $N = 2$ extra dimensions would provide tangible evidence of quantum gravity at the TeV scale. Parton-parton scattering in $p\bar{p}$ collisions, and in νN scattering events, are two proposed production methods. If $N = 2$ black holes exist, one should see their copious production and decay at the LHC, and at a lower rate in neutrino arrays such as AMANDA/ICECUBE. Because of differences in resolution and background levels, the LHC and neutrino telescopes have their own advantages—high event rates are usually sacrificed for clean signal. As of this writing, no black holes have been seen in neutrino arrays; studies at the LHC have yet to be done.

References

- [1] S. Inhinose. To Appear in *Class. Quan. Grav.*
- [2] G. Gonzalez. NEB-X, tenth Greek Relativity Meeting, 2003.
- [3] A. Dedes, S. Heinemeyer, P. Teixeira-Dias, and G. Weiglein. Technical Report 99-368, CERN, December 1999.
- [4] K. Hagiwara et al. The review of particle physics. *Phys. Rev. D*, 66:010001, 2002.
- [5] N. Arkani-Hamed, S. Dimopoulos, and G. Dvali. *Phys. Lett.*, B249:263–272, 1998.
- [6] A. Ringwald. *Fortsch. Physics*, 51:830–835, 2003.
- [7] Y. Uehara. *Prog. Theor. Phys.*, 107:621–624, 2002.
- [8] M. Cavagla. *Int. J. Mod. Phys.*, A18:1843–1882, 2003.
- [9] M. Cavagla, S. Das, and R. Maartens. *Class. Quant. Grav.*, 20:L205–L212, 2003.
- [10] A. Kotwal and S. Hofmann. Technical report, Dept. of Physics, Duke University, Durham, NC and Institut für Theoretische Physik, J. W. Goethe Universität, Germany, 2002.
- [11] S. Dimopoulos and G. Landsberg. *Phys. Rev. Lett.*, 87:161602, 2001.
- [12] T. Han, G. Kribs, and B. McElrath. *Phys. Rev. Lett.*, 90:031601, 2003.
- [13] A. Dighe, M. Keil, and G. Raffelt. *JCAP*, 306(5), 2003.
- [14] C. Harris, P. Richardson, and B. Webber. *JHEP*, 308(33), 2003.
- [15] O. Biebel, M. Binder, et al. Technical Report LMU-ETP-2003-01, The ATLAS collaboration, July 2003.
- [16] M. Drees, E. Ma, P. Pandita, et al. *Phys. Lett.*, B433:346–354, 1998.
- [17] P. Bhattacharjee and N. Gupta. To Appear in *Astropart. Phys.*, 2003.
- [18] E. Ahn, M. Ave, M. Cavaglia, and A. Olinto. *Phys. Rev.*, D68:043004, 2003.
- [19] L. Evans et al., 2003.
- [20] C. Amsler. *Rev. Mod. Phys.*, 70:1293, 1998.
- [21] L. Anchordoqui, J. Feng, H. Goldberg, and A. Shapre. Technical Report NUB-3239-Th-03, Department of Physics and Astronomy, Northeastern University, July 2003.